Solvent Effect in Hydrogenolysis of Xylitol over Bifunctional Ru/MnO/C Catalysts under Alkaline-Free Conditions

M. Riviere, N. Perret, D. Delcroix, A. Cabiac, C. Pinel, M. Besson

Solvent Effect in Hydrogenolysis of Xylitol over Bifunctional Ru/MnO/C Catalysts under Alkaline-Free Conditions

Maxime Rivière[1], *Noémie Perret*[1], *Damien Delcroix*[2], *Amandine Cabiac*[2], *Catherine Pinel*[1], *Michèle Besson*[*1].

[1]Univ Lyon, Univ Claude Bernard, CNRS, IRCELYON, UMR5256, Institut de recherches sur la catalyse et l'environnement de Lyon, 2 Avenue Albert Einstein, 69626 Villeurbanne, France

[2]IFP Energies nouvelles, Rond-Point de l'Echangeur de Solaize, BP 3, 69360 Solaize, France

*to whom correspondence should be addressed. Email: michele.besson@ircelyon.univ-lyon1.fr Tel: +33 472 445 358.

ABSTRACT

The hydrogenolysis reaction of biomass-derived xylitol to glycols and glycerol has been carried out in different aqueous solvents over a bifunctional Ru/MnO/C catalyst under alkaline-free conditions at 60 bar H_2 and 200°C. In pure water, the retro-aldol reaction takes place. However, decarbonylation and epimerization are the dominant reactions and produce C4 and C5 alditols, which limits the overall selectivity to glycols and glycerol (30%). When 90:10 vol.% water:1,4-dioxane and water:2-PrOH solutions are used as solvent, the product distribution is very similar to the one in water. Meanwhile, in 90:10 vol.% water:primary alcohol (ROH with R = Me, Et, nPr, nBu) the overall selectivity to glycols and glycerol is greatly enhanced (up to 70%), whereas the selectivity to C4 and C5 alditols is reduced. In a solution with higher MeOH proportion of 20 vol.%, the glycols are detected with even higher selectivity, however, some deactivation of the catalyst is observed. TGA analysis of the used catalysts shows that during the process some coke is deposited on the catalyst via a dehydrogenation step of ROH. The coke selectively poisons the Ru sites that are active for the undesired reactions of decarbonylation and epimerization.

KEYWORDS hydrogenolysis, glycols, biomass-derived xylitol, bifunctional Ru-MnO catalyst, deactivation

INTRODUCTION

Inedible biomass is considered to be a promising sustainable alternative resource to supply the increasing demand for carbon-based chemicals, likewise to avert the environmental issues and the dependence on fossil ressources.[1,2] Cellulose and hemicelluloses are the most abundant renewable sources of carbon. Much attention has been given to their conversion to sorbitol and xylitol by hydrolysis and subsequent catalytic hydrogenation in aqueous phase, since alditols are versatile building blocks, precursors of various valuable compounds, including glycols.[3] Ethylene glycol (EG) and propylene glycol (PG) are used in a large number of industrial processes: as raw materials in heat-transfer fluids industries, as monomers in the manufacture of polyester resins for clothes, and in cosmetic, pharmaceutical and packaging industries.[4,5] Currently produced in high volume (25 million tons in 2015) from petro-ethylene and propylene via epoxides,[6] glycols produced by hydrogenolysis of biomass-derived polyols get a growing interest.

Generally, hydrogenolysis of xylitol and sorbitol requires a supported-noble or transition metal catalyst (i.e., Ru, Ni or Cu) and a homogeneous base (i.e., $Ca(OH)_2$, NaOH, $Ba(OH)_2$) to catalyze the C – C and C – O bond cleavages. The reactions are performed in aqueous phase under harsh conditions, namely 160 – 230°C and 40 – 120 bar H_2. Through the decades of investigations, the selective catalytic hydrogenolysis of sorbitol and xylitol has improved as concerns the reaction pathways and mechanisms.[7–10] The hydrogenolysis is a complex system consisting of several reaction steps. In the simplified and most widely accepted scheme for hydrogenolysis of xylitol

in the presence of a soluble base, the reaction is initiated by the dehydrogenation of xylitol to the corresponding aldose (i.e., xylose) or ketose (i.e., xylulose or 3-pentulose) over metallic sites and then selective C – C bond cleavage reaction takes place catalyzed by the base via retro-aldol reaction to C2 and C3 intermediates depending on the initial dehydrogenation position (**Scheme 1**).[11,12] These intermediates are then hydrogenated on the metallic sites to the target glycols and glycerol. However, several side-reactions may occur: (i) decarbonylation of the terminal carbonyl bond on the metal which generates CO and C4 compounds (i.e., threitol)[13], (ii) epimerization which forms arabitol and adonitol[8], and (iii) Cannizzaro-type reaction catalyzed by a base which yields lactate.[13]

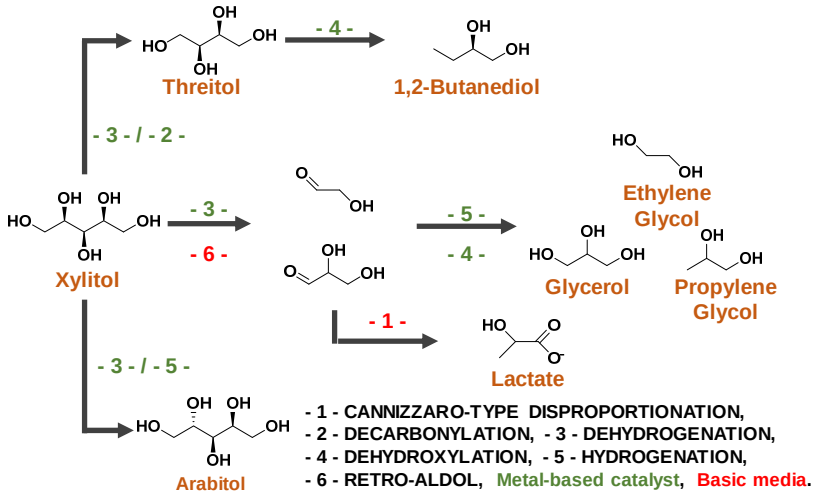

Scheme 1. Simplified reaction scheme for xylitol hydrogenolysis over metal-based catalyst under alkaline conditions and main reactions involved.

The hydrogenolysis of xylitol (10 wt.% aqueous solution, 200°C, 60 bar H_2) over 90%Cu-SiO_2 catalyst in the presence of $Ca(OH)_2$ generated yields of glycols and glycerol of 5 – 60%.[14,15] Ni-based catalysts, such as 6%Ni-NaY, achieved high conversion of sorbitol in the presence of $Ca(OH)_2$ (15 wt.% aqueous solution, 220°C, 60 bar H_2) and a 70% selectivity to glycols and glycerol.[16] A high overall selectivity to glycols and glycerol of 85% was recently reported over a

10%Ni80%Cu-SiO_2 catalyst for the hydrogenolysis of xylitol in the presence of $Ca(OH)_2$ (10 wt.% aqueous solution, 200°C, 80 bar H_2).[17] The Ru-based catalysts appear to be the most active catalysts. High conversions of sorbitol were reported over 3%Ru/carbon nanofibers (86%) and 3%Ru/C (71%) in the presence of CaO (20 wt.% solution, 220°C, 80 bar H_2, 4 h) with a selectivity to glycols and glycerol of 61% and 29%, respectively.[18] Sun and Liu[11] reported a production of 67% glycols and glycerol over 4%Ru/C catalyst in the presence of $Ca(OH)_2$ (10 wt.% xylitol, 200°C, 40 bar H_2) and, in our previous work, we reported an activity of 223 h^{-1} with a selectivity to glycols and glycerol of 57% over 2.9%Ru/C catalyst in the presence of the same base (10 wt.% xylitol, 200°C, 60 bar H_2).[19]

However, the use of large amounts of inorganic homogeneous base limits the economic viability of the process, due to the formation of lactate at the expense of PG and the final neutralization and separation step requirements that generate high amounts of salt.[20] Therefore, recent studies explored the hydrogenolysis reaction of alditol aqueous solutions under alkaline-free conditions over bifunctional catalysts combining both metallic and basic properties. A selectivity to glycols and glycerol of approximately 80% with limited formation of lactic acid was obtained at 68% conversion of sorbitol over Ni-MgO (200°C, 40 bar H_2),[21] while a 48% selectivity was achieved over Ni-Ru/$Ca(OH)_2$ catalysts.[22] Other formulations such as Ni-Mg-Al, Cu/CaO-Al_2O_3 and Ni-CaO/C catalysts were reported for sorbitol or xylitol under base-free conditions with a selectivity to glycols and glycerol of 60%, 73% and 69%, respectively.[20,23,24] In our earlier work, we demonstrated that a 3.1%Ru/MnO(4.5%)/C catalyst was very active (220 h^{-1}) and selective to glycols and glycerol (32%) for the hydrogenolysis of xylitol under base-free conditions (10 wt.%, 200°C, 60 bar H_2).[19] Moreover, the production of glycols was limited by the competition between the desired retro-aldol and the side-reactions in aqueous solution.

Indeed, Ru-based catalysts showed excessive C-C bond cleavage and formed light alkanes under base-free conditions (15% of products in gas phase). As far as we know, only water has been used as solvent for hydrogenolysis of xylitol and little attention has been given to the effect of the solvent on the reaction. It is worth noting that the use of water:ethanol or water:2-propanol (H_2O:EtOH or H_2O:2-PrOH) solvents for the hydrogenation of xylose to xylitol resulted in higher rates.[25] Furthermore, a Cu-ZnO catalyst exhibited a higher activity for hydrogenolysis of glycerol in EtOH and MeOH, which might be due to the in situ generation of hydrogen from the solvent.[26]

In the present work, the reaction was carried out over a Ru/MnO/C catalyst in water:dioxane and water:alcohol mixtures (MeOH, EtOH, 1-PrOH, 2-PrOH, and 1-BuOH). This catalyst demonstrated a bifunctional character with basic and metallic sites to perform the reaction in base-free aqueous solution, while exhibiting high activity and selectivities.[19] We investigated the impact of the reaction media in an attempt to improve its performances. Moreover, water:alcohol mixtures should have low environmental impact, according to the green solvent definition by Fischer et al.[27]

EXPERIMENTAL SECTION

Materials. D-Xylitol (99%), 2-propanol (>99.5%), 1-butanol (>99.5%), methyl β-D-xylopyranoside (>99%) were purchased from Sigma Aldrich, methanol (>99.9%) and 1,4-dioxane from Carlo Erba, ethanol (99.5%) from Elvetec, 1-propanol (98%) from VWR Chemicals, $Ru(NO)(NO_3)_3.xH_2O$ (Ru > 31.3 wt.%) was purchased from Alfa Aesar and $Mn(NO_3)_2.4H_2O$ (98%) from Merck. Activated carbon L3S was provided by CECA. Hydrogen

(H_2 > 99.5%), argon (Ar > 99.5%), 1% v/v O_2/N_2, and 5% v/v CO_2/He gases were from Air Liquide.

Catalysts Preparation. The bifunctional 3.1%Ru/MnO(4.5%)/C catalyst (3.1 and 4.5 are the wt.% of Ru and Mn, respectively) was prepared by the successive wet impregnation method.[19] Typically, an aqueous solution of the Mn precursor at the desired concentration was added to the suspension of active carbon in water within a round-bottom flask. After stirring for 6 h at RT, water was removed by evaporation and the resulting powder was dried at 110°C overnight and calcined at 200°C (2°C min^{-1}) for 4 h under air flow (100 mL min^{-1}). Subsequently, the MnO/C powder was wet impregnated with an aqueous solution of the desired amount of Ru precursor. After evaporation, the solid was reduced at 450°C (2°C min^{-1}) for 3 h under H_2 flow (100 mL min^{-1}) and, finally, passivated under 1% v/v O_2/N_2 gas flow for 30 min at RT. The monometallic x%Ru/C catalyst was synthetized using the same impregnation procedure and reduction treatment.

Catalyst Characterization. The metal loadings of the catalysts were determined after dissolution in *aqua regia* at 150°C for 12 h and analysis by inductively coupled plasma-optical emission spectroscopy (ICP-OES, Activa Jobin-Yvon). The crystallite phases were determined by X-ray diffraction (XRD, Brucker D8A25) with CuK_α radiation and multi-channel fast detector LynxEye while the specific surface areas were determined by N_2 physisorption isotherms (ASAP 2020) at 77 K after thermal treatment (350°C for 7 h under vacuum 10^{-4} mbar). The amount of basic sites on the catalyst surface were determined by temperature-programmed desorption (TPD, Belcat-M) of CO_2. Typically, the reduced sample was pre-treated in He gas (50 mL min^{-1}) at 500°C for 1 h and then cooled to 100°C, and saturated with 5% v/v CO_2/He. The TPD profiles were recorded using a thermal conductivity detector (TCD) while heating the sample from 100°C

to 500°C under a continuous flow of He (50 mL min^{-1}). The used catalysts were analyzed by thermogravimetric analysis coupled with differential thermal analysis (TGA-DTA, Star^e System Mettler Toledo). TEM images were taken by using a JEOL 2010 instrument operated at 200 keV. The average size of Ru particles was determined by measuring approximately 300 particles distributed randomly in the images.

Catalytic testing. Hydrogenolysis of xylitol was carried out in a Hastelloy Parr autoclave (300 mL) at a stirring speed of 1000 rpm. In a typical run, 135 mL of 10 wt.% xylitol solution and 0.5 g catalyst were introduced into the autoclave. After purging with Ar, the reactor was heated to the reaction temperature. It was then pressurized with H_2, which corresponded to the reaction time $t = 0$. The same procedure was used for the catalytic tests in solvent mixtures. For instance, for 90:10 vol.% water:MeOH solvent, 15 g of xylitol were introduced in 121 mL water blended with 14 mL MeOH.

During the reaction, liquid samples were periodically collected through a sampling valve and filtered through polyvinylidene fluoride (PVDF) membranes (0.45 μm) before analysis. After reaction, the reactor was cooled to RT and depressurized to atmospheric pressure. The catalyst was separated by vacuum filtration through PVDF membranes (0.45 μm) and dried at 70°C under N_2 atmosphere.

The products in the liquid samples were identified and quantified using two different HPLC instruments (Shimadzu) connected to refractive index diffraction (RID10A) and UV detectors (SPD-M10A). Moreover, the gaseous phase was collected at the end of reaction at RT in a gas collecting bag and analyzed by gas chromatography (μ-GC SRA, Agilent) using a catharometric detector and connected to a mass spectroscopy module (MS 5975, Agilent), as described previously.[19] The total organic carbon (TOC) in pure water solvent was measured using a TOC

analyzer (Shimadzu TOC-VCHS equipped with ASI-automatic sampler) and compared to initial TOC to estimate the formation of gaseous products. Conversion, selectivities (on a carbon basis %), and initial reaction activity ($mol_{xylitol}\ mol_{Ru}^{-1}\ h^{-1}$) were calculated as previously.[19]

RESULTS AND DISCUSSION

Catalyst Characterization. The metal loadings, the specific surface areas, and the total amount of basic sites of the catalysts were determined previously and are summarized in **Table S1**.[19] The XRD pattern (**Fig. S1**) showed that the MnO phase was obtained with an average crystallite size of 14 nm. No peak attributed to Ru was detected over Ru/C and Ru-MnO/C, suggesting well dispersed Ru particles. 3.1%Ru/MnO(4.5%)/C catalyst exhibits a higher basic sites amount (355 μmol g^{-1}, determined by CO_2-TPD) than 2.9%Ru/C (261 μmol g^{-1}), according to Ishikawa et al.[28] The TEM images of Ru/C and 3.1%Ru/MnO(4.5%)/C catalysts are shown in **Figure 1**. Ru nanoparticles on Ru/C are well dispersed over the active carbon surface with a mean particle size of 1.6 nm. On the bifunctional Ru/MnO/C catalyst, large particles (main size around 25 nm) were attributed to MnO by EDX analysis and small particles (2.1 nm) to Ru. The Ru particles are either directly on the support or on large particles of MnO.

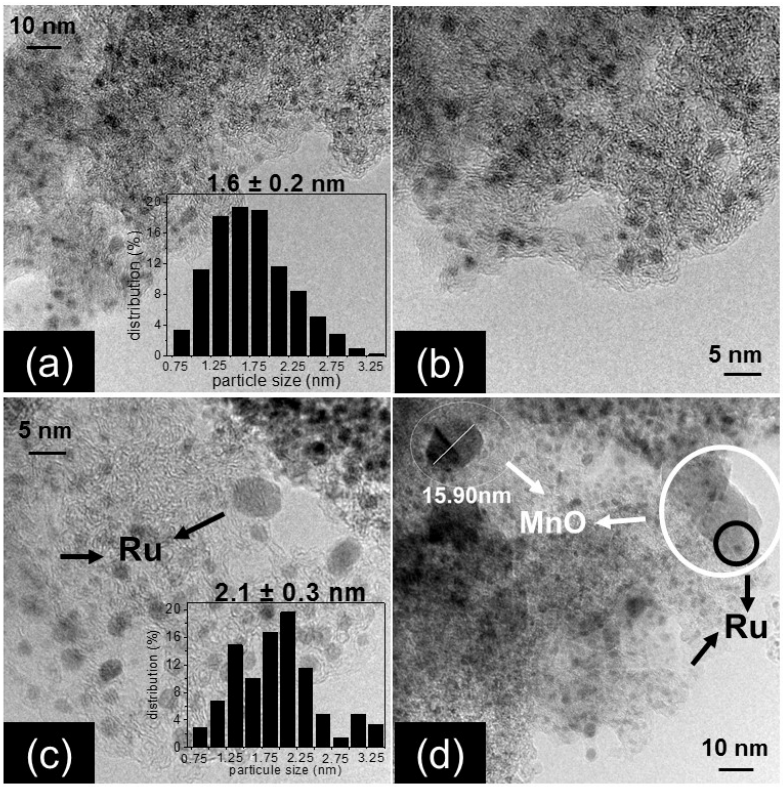

Figure 1. TEM images of monometallic 2.9%Ru/C [(a) and (b)] and bifunctional 3.1%Ru/MnO(4.5%)/C [(c) and (d)] with the Ru particles size distribution.

Hydrogenolysis of xylitol in water:dioxane or alcohol solvents. Hydrogenolysis of xylitol was conducted in different solvents at 200°C and 60 bar H_2 over Ru/MnO/C catalyst under alkaline-free conditions. Some physicochemical properties of the solvents used are given in **Table S2**.

The temporal evolutions of the conversion of xylitol, products distribution, and TOC measurements in liquid phase are shown in **Figure 2** for the reaction in pure water, taken as a reference experiment. Xylitol was fully converted after 30 h of reaction. The major products in the liquid phase were propylene glycol (PG), ethylene glycol (EG), glycerol (GLY), C4 alditols (mainly threitol and a small amount of erythritol). Butanediols (BDO), notably 1,2-BDO, and C5 alditols (arabitol and traces of adonitol) were also identified. The reaction profile revealed that

most products in liquid phase attained a maximum concentration at 80% xylitol conversion after 9 h. Afterwards, the concentrations decreased gradually for EG, GLY, C4 and C5 alditols, whereas the concentrations of PG and BDO were still continuously increasing. The decline of TOC in liquid phase indicates that a large amount of the products was transformed into alkanes and CO_2 in the gas phase. The major products in gas phase were, from the highest to lowest amount (carbon basis): methane, ethane, propane, CO_2, and traces of butane and pentane.

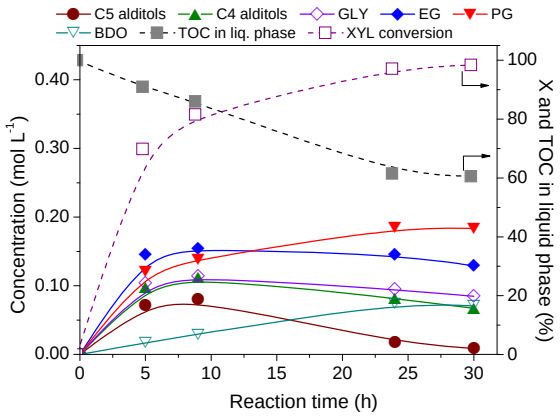

Figure 2. Temporal evolution of conversion (X), TOC measure, and concentrations during hydrogenolysis of xylitol in pure water over 3.1%Ru/MnO(4.5%)/C. Reaction conditions: xylitol 0.7 mol.L^{-1} (10 wt.%), 135 mL water, 0.5 g 3.1%Ru/MnO(4.5%)/C, 60 bar H_2, 200°C.

The results confirmed that several reactions were taking place and were competing over the bifunctional catalyst in water under alkaline-free conditions.[19,23,24,29] The glycols and glycerol were mainly produced from the retro-aldol reaction of xylose or xylulose, which are intermediates from xylitol. After the initial step of dehydrogenation of the alditol, the retro-aldol reaction is favored by the basic sites on the catalyst.[20,24] Herein, dehydrogenation of xylitol occurred over metallic Ru, and the MnO species over the surface provide the basic sites. Moreover, Hausoul et al.[30] demonstrated that under these reaction conditions of temperature and pressure, Ru particles were also responsible for side-reactions of epimerization, decarbonylation, and dehydroxylation to yield the C5 alditols, C4 alditols, and BDO, respectively. The large

extent of decarbonylation and dehydroxylation reactions produced light alkanes that were detected at the end of the reaction. Thus, while Ru is required along with MnO species for the retro-aldol reaction, the Ru particles also inevitably favor the side-reactions. The use of other solvents than pure water was examined in an attempt to modify the catalyst performance. Hydrogenolysis of xylitol was first run in the presence of 90:10 vol.% H_2O:1,4-dioxane solvent in order to investigate the influence of an aprotic and non-polar compound, although we were aware of the non-sustainability of dioxane (**Table S2**). Since 1,4-dioxane is stable under H_2 pressure at high temperature in the presence of Ru-based catalysts, it is often used as solvent for hydrogenation reactions.[31,32] As shown in **Figure 3.a**, xylitol conversion was complete after 30 h and a very similar product distribution as a function of time was observed as the one in pure water (**Figure 2**). The addition of 1,4-dioxane to water did not affect the activity and the product distribution. Less than 10% of 1,4-dioxane was removed from the liquid phase during the reaction, more particularly in the first few hours because of its partial vaporization under the reaction conditions. Therefore, the use of 1,4-dioxane as aprotic and non-polar solvent did not limit the side-reactions.

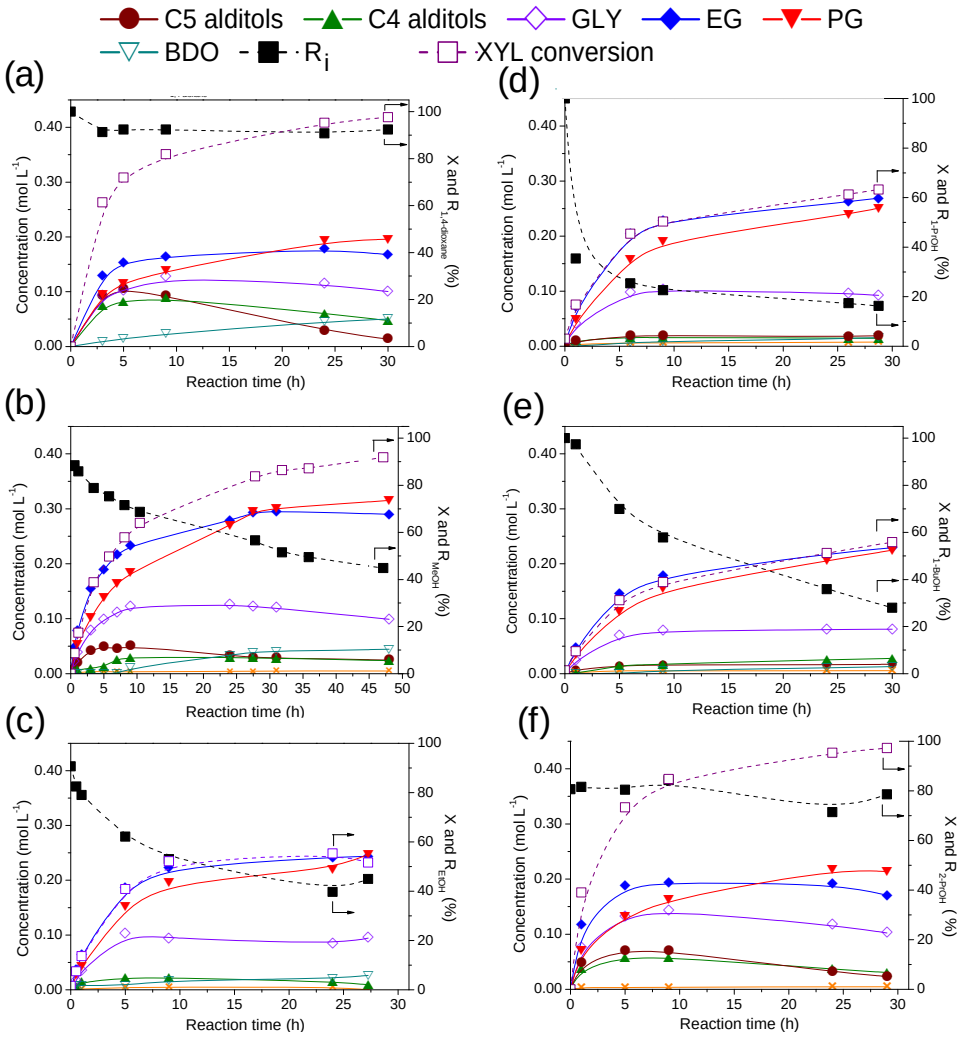

Figure 3. Xylitol hydrogenolysis over 3.1%Ru/MnO(4.5%)/C in different solvents: (a) 90:10 vol.% H_2O:1,4-dioxane, (b) H_2O:MeOH, (c) H_2O:EtOH, (d) H_2O:1-PrOH, (e) H_2O:1-BuOH, (f) H_2O:2-PrOH. X: xylitol conversion, R_i: ratio of recovered dioxane or alcohol concentration to the initial concentration. Reaction conditions: xylitol 0.7 mol.L^{-1} (10 wt.%), 135 mL 90:10 vol.% H_2O:organic solvent, 0.5 g 3.1%Ru/MnO(4.5%)/C, 60 bar H_2, 200°C.

To survey the impact of primary alcohols (MeOH; EtOH; 1-PrOH; 1-BuOH), they were added as 10 vol.% concentration in water. Primary alcohols are polar with different surface tensions and H_2 solubilities (**Table S2**). The reaction profiles are shown in **Figure 3.b-e,** and the data for the activities and selectivities to the main products are summarized in **Figure 4**. The results differed strongly compared to pure water. First, a significant impact was observed on the reaction

rates. The activity decreased from 220 h^{-1} to 71 h^{-1} in H_2O:MeOH, 56 h^{-1} in H_2O:EtOH, 57 h^{-1} in H_2O:1-PrOH and 39 h^{-1} in H_2O:1-BuOH (**Figure 4**). These results were unlike those reported by Mikkola et al.[25] for hydrogenation of xylose to xylitol: the catalytic activity over Raney Ni in a 75:25 vol.% H_2O:EtOH solvent (80 – 130°C; 40 – 80 bar H_2) was twice the activity in water, suggesting that the enhancement of H_2 dissociation on Ni active sites was driven by the increasing solubilization of H_2 in the H_2O:EtOH solvent. However, the H_2 solubilities are similar in H_2O:ROH (90:10) mixtures or in pure H_2O solvent (**Table S2**). Moreover, we assumed that the solubility of H_2 was not the limiting factor in the present system, since the reactor was continuously fed with H_2 to keep the pressure constant and the activity decreased with increasing solubility. Thus, we suggest that the drop of activity might be the consequence of competitive adsorption of the primary alcohol and xylitol on active sites.

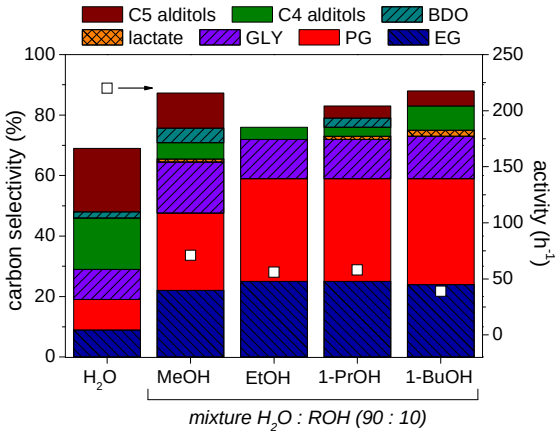

Figure 4. Hydrogenolysis of xylitol over 3.1%Ru/MnO(4.5%)/C in water and 90:10 vol.% H_2O:primary alcohol solvent. Selectivities at 60% xylitol conversion. Reaction conditions: xylitol 0.7 $mol.L^{-1}$ (10 wt.%), 135 mL 90:10 vol.% H_2O:ROH solvent, 0.5 g 3.1%Ru/MnO(4.5%)/C, 60 bar H_2, 200°C.

Meanwhile, the selectivity to glycols was greatly improved (**Figure 4**). At 60% xylitol conversion, the selectivities to EG and PG increased from 9% and 10% in pure water to 22% and 25% in 90:10 vol.% H_2O:MeOH solvent, respectively. The selectivity to GLY increased slightly from 10 to 15%, while the one to BDO remained roughly constant at 5%. On the other hand, the

overall selectivity to C4 and C5 alditols dropped from 38% to 10%. Additionally, the carbon balance in liquid phase was close to 90% in presence of alcohol, which suggests a low production of alkanes.

In the other water:primary alcohol (EtOH; 1-PrOH and 1-BuOH) solvents the selectivities to glycols detected were even higher (25% and 34% to EG and PG, respectively) than in water:MeOH, whereas the overall selectivity towards BDO, C4, and C5 alditols decreased to 10%. It is worth to mention that in the case of H_2O:EtOH quantification of C5 alditols could not be done, since arabitol and EtOH were co-eluted on the HPLC column, however, we presumed that arabitol formation followed the same trend as in the other runs. Therefore, the present results showed that the use of a 90:10 vol.% water:primary alcohol mixture greatly affected the performance of the Ru/MnO/C catalyst in terms of activity and selectivity. Earlier on we suggested two types of active sites. The number of Ru sites responsible for epimerization and decarbonylation seemed to have decreased, while the ability of MnO species close to Ru associated with the cleavage of the C – C bonds of xylitol to glycols and glycerol was not affected.

Nevertheless, these results (**Figure 3.b-e**) revealed two important drawbacks associated with the use of primary alcohol: (i) a large fraction of the alcohol was no more analyzed in the liquid phase, and (ii) a deactivation of the catalyst was evidenced. Indeed, during the heating period up to the reaction temperature, the concentration in liquid phase of alcohol decreased: by 10% for MeOH and EtOH, and up to 60% for 1-PrOH. This was due to the vaporization of alcohol to the gaseous phase. Then, the fraction of alcohol in the solvent still decreased during the reaction. One may note that the loss of primary alcohol in the mixed solvent should increase the concentrations of the analyzed products, and thus enhance the selectivity to the different

products. Nevertheless, this overestimation could be neglected owing to the low volume of alcohol (10 vol.%) in the solvent. Furthermore, as mentioned above, a slow-down of xylitol conversion was observed after 9 h, followed by a pseudo-plateau, essentially for EtOH, 1-PrOH and 1-BuOH. Xylitol conversion was not total even upon extension of the reaction time. The products and solvent concentrations remained stable in the liquid phase.

The influence of the fraction of alcohol in the solvent was investigated using MeOH, owing to the lower deactivation when using MeOH. The hydrogenolysis of xylitol experiments were performed over Ru/MnO/C with different water:MeOH ratios (MeOH: 5, 10 and 20 vol.%). The data of activity and selectivity to the main products are shown in **Figure 5**. The activity dropped from 220 h^{-1} in water to 90 h^{-1} in 95:5vol.% H_2O:MeOH and it further decreased to 43 h^{-1} with an increase of MeOH concentration to 20 vol.%, confirming the competitive adsorption on the active sites of MeOH and xylitol. As shown in the graphic, the combined selectivity to glycols increased gradually as the MeOH concentration increased. Starting at 22% (EG 10%, PG 12%) in pure water, the selectivity to glycols increased to 39% (EG 19%, PG 20%) in 95:5 vol.% H_2O:MeOH solvent and to 61% (EG 23%, PG 38%) in 80:20 vol.% H_2O:MeOH. Concurrently, the overall selectivity to C5 and C4 alditols was significantly reduced from 23% and 18% to 4% and 3%, respectively, and the selectivity to glycerol and BDO remained constant at 13% and 5%, respectively. Thus, it was confirmed that with increasing MeOH fraction in the solvent, the retro-aldol reaction was clearly the dominant reaction at the expense of the undesired decarbonylation and epimerization reactions. Xylitol conversion was complete after 24 h in water, whereas it was never total in H_2O:MeOH solvent (**Figure S3**). The concentration of xylitol was limited at ca. 0.10 mol L^{-1} after 24 h, i.e. 85% conversion, in 95:5 vol.% H_2O:MeOH. The pseudo-plateau was observed at lower conversion (60%) in 80:20 vol.% H_2O:MeOH.

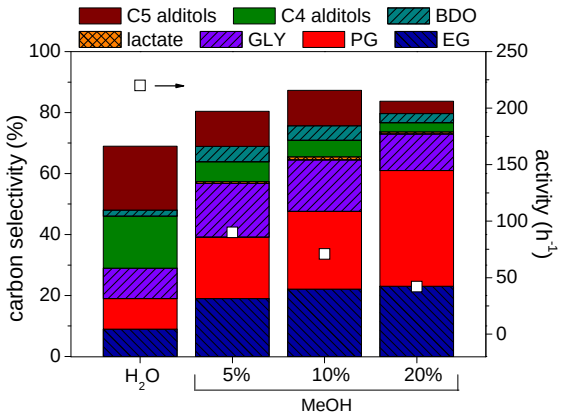

Figure 5. Activity and selectivities at 60% conversion during hydrogenolysis of xylitol over 3.1%Ru/MnO(4.5%)/C in H_2O:MeOH solvent. Reaction conditions: xylitol 0.7 mol.L^{-1} (10 wt.%), 135 mL solvent, 0.5 g 3.1%Ru/MnO(4.5%)/C t, 60 bar H_2, 200°C.

Further insights in catalyst deactivation. The catalytic deactivation can be related with textural modifications or poisoning of the active sites.[33] The X-Ray diffraction patterns of the used catalysts after reaction revealed a slight increase of Ru crystallite size and disappearance of the diffraction peaks attributed to MnO (**Figure S1**). These similar results in water or in water:alcohol solvent suggest that the textural modifications were not responsible for the deactivation. Therefore, the deactivation was likely due to the presence of the alcohol. In the same way as xylitol, the alcohol can be dehydrogenated on the Ru active sites and yield the corresponding aldehyde. However, the aldehydes (formaldehyde to butyraldehyde) were not observed, neither in the liquid phase nor in the gas phase. Hence, we concluded that the deactivation was due either to the poisoning of Ru active sites by intermediate species from the alcohol (i.e. hydroxyalkyl or alkoxy species) or to a side-reaction taking place between the alcohol and an intermediate from xylitol. According to computational DFT studies on the dehydrogenation of primary alcohols over Ru or Pt sites, the desorption of alkoxy species is the determining step and the energies are the same whatever the C_2-C_4 alkoxy species.[34–36] MeOH behaved differently as compared to the other primary alcohols, since its adsorption energy was

found higher. According to the present results (**Figure 3**) the deactivation was less important in the presence of MeOH, suggesting that the methoxy intermediate would be easier to transform to methane. This was confirmed by the high concentration of CH_4 analyzed in the gas phase. The other explanation for deactivation is the occurrence of side-reactions between the alcohol and a derivative issued from xylitol over the Ru active site which will poison the catalyst and limit the access to the surface. Iglesias et al.[37] noted for instance the formation of an alkyl-xyloside intermediate during dehydration of xylose in MeOH or EtOH solvent at 150°C (**Figure S2**). This intermediate could be generated under our reaction conditions under mild-acid conditions (pH 4.5-6.5) and deactivate the catalyst, even though it was not detected in the liquid phase.

We further investigated the effect of the alcoholic solvent and of these possible intermediates on the deactivation of Ru/MnO/C catalyst. First, in order to identify the poisoned active sites and the ROH degradation sites, catalytic tests were performed over the monometallic Ru/C catalyst, the MnO/C solid, or the bifunctional Ru/MnO/C catalyst in 90:10 vol.% H_2O:MeOH solvent in the presence or in the absence of xylitol (**Figure 6.a**). Regarding MeOH removal from the liquid phase, at $t = 0$ after the 45 min heating period, 10% of methanol was systematically lost from the liquid phase, which corresponds to the vaporization of a fraction of MeOH. Then, as expected MnO/C was not active for MeOH transformation. Conversely, in the presence of Ru/C or Ru/MnO/C, removal of MeOH was in the range of 50% to 90% after 24 h, and methane was the sole product in the gas phase. Over Ru/C, whether xylitol was present or not, conversion of MeOH was the same (c.a. 50%), which suggests preferential adsorption of MeOH on the surface. Conversely, over Ru/MnO/C catalyst, degradation was lower in the presence of xylitol (50% vs. 90%), which implies higher adsorption of xylitol. Moreover, as mentioned above, the addition of MeOH influenced the rate of xylitol conversion (**Figure 6.b**). The initial rate decreased by a

factor ca. 17 in the presence of Ru/C vs. a factor ca. 3 in the presence of Ru/MnO/C. This fact confirms distinct active sites on both catalysts with different affinity for MeOH and xylitol.

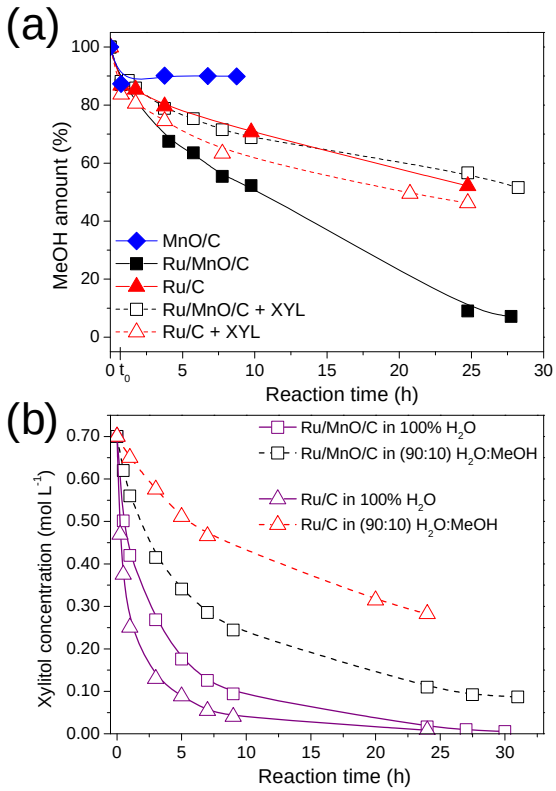

Figure 6. Influence of the catalyst on deactivation. (a) MeOH consumption as a function of time in 90:10 vol.% H_2O:MeOH in the absence or presence of xylitol. (b) Evolution of xylitol concentration in water or 90:10 vol.% H_2O:MeOH.

In order to further understand the deactivation phenomenon and to observe the possible deposition of carbonaceous species on the surface of used catalyst, TGA – DTA analysis of used catalysts was performed under air flow.[33,38] After reaction in water, two major weight losses which generated heat were recorded for the used Ru/MnO/C catalyst: one at 80°C (10% weight loss) attributed to the desorption of physisorbed water and a second one at 350 – 425°C (90% weight loss) (**Figure 7**). We assumed that the second one corresponded to the total combustion of active carbon support, principally composed of polyaromatic carbons.[39] At the end of the analysis, only Ru and Mn oxides remained and represented 7% of the initial mass. After reaction

in 80:20 vol.% H_2O:MeOH, the same weight loss was recorded at 350 – 425°C and attributed to the combustion of support. Nonetheless, another weight loss of 20% appeared at lower temperature (250°C) along with a heat peak suggesting another combustion reaction. This suggests the presence of a "soft" coke, constituted of oligomers and containing oxygen atoms in their chain. The tendency for TGA-DTA of used catalysts after the catalytic tests in 90:10 vol.% water:alcohol solvents was very similar (**Figure S4**) to that observed after the experiment in water: MeOH (**Figure 7**). Since this weight loss was not observed on the used catalyst after reaction in pure water, we may ascertain that the coke originated from species issued from the alcoholic solvent.

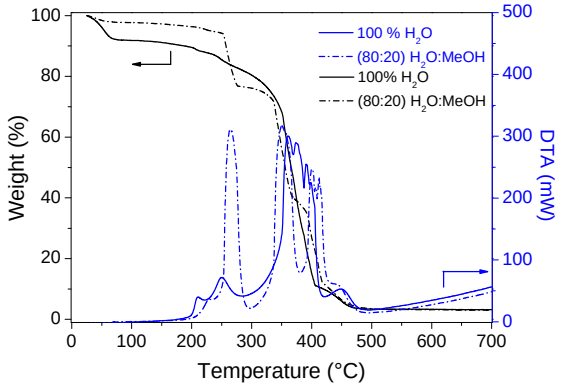

Figure 7. TGA-DTA under air flow of used 3.1%Ru/MnO(4.5%)/C after xylitol hydrogenolysis in 100%H_2O and (80:20) H_2O:MeOH mixture. Reaction conditions: xylitol 0.7 mol.L^{-1} (10 wt.%), 135 mL solvent, 0.5 g 3.1%Ru/MnO(4.5%)/C, 60 bar H_2, 200°C.

The coke may be initiated by the dehydrogenation of MeOH, even though formaldehyde was not detected in the liquid or the gas phase, or by the degradation of methyl xyloside possibly formed as intermediate. To verify these hypotheses and to identify the species responsible for the catalyst deactivation, xylitol hydrogenolysis was carried out over Ru/MnO/C in the presence of acetaldehyde (CH_3CHO) or methyl xyloside (**Table 1**). The addition of a small amount (1 g) of methyl xyloside to pure water resulted in a similar activity of the Ru/MnO/C catalyst as in 90:10 vol.% H_2O:MeOH (approximately 224 h^{-1}) and conversion of xylitol was complete after 30 h.

Also, it did not affect the product distribution, except a slight increase of the combined selectivity to glycols and glycerol from 34% to 38%, and those to C5 and C4 products from 41% to 44%. Simultaneously to xylitol conversion, methyl xyloside was entirely converted after 9 h. Therefore, we concluded that methyl xyloside, if formed during the reaction in H_2O:MeOH solvent, could not be responsible for the poisoning. On the contrary, the Ru/MnO/C catalyst was completely inactive in aqueous solution containing 10 vol.% acetaldehyde (**Table 1**). No xylitol conversion was detected after 9 h of reaction. The ratio of recovered acetaldehyde to the initial concentration was 23% after 1 h. Part of the aldehyde was removed by vaporization in the gas phase. Hydrogenation and Cannizzaro-type reactions of acetaldehyde generated small amounts of EtOH and acetic acid (as detected by HPLC) which contributed to this loss, as well as coke formation. After a few hours of reaction, acetaldehyde concentration remained constant and no modification in the product distribution was noted. Taking into account that the poisoning of the catalyst occurred to some extent in H_2O:EtOH and dramatically in H_2O:CH_3CHO solvent, it was suggested that an intermediate formed from the alcohol or the aldehyde was responsible for the coke formation that significantly influenced the reaction.

Table 1. Hydrogenolysis of xylitol in different solvents and in presence or not of methyl xyloside over 3.1%Ru/MnO(4.5%)/C.[a]

Reaction medium (%vol.%)	**Activity** (h^{-1})	**Carbon selectivity**[b] **(%)**						R_i[d] (%)
		EG	**PG**	**GLY**	**LA**	**C_4 products**[c]	**C_5 alditols**	
100% H_2O	220	10	12	12	< 1	18	23	-
CH_3-Xylo.[e]	224	12	12	14	< 1	20	24	0
EtOH : H_2O (10 : 90)	56	25	34	13	< 1	4	0	40
CH_3CHO : H_2O (10 : 90)	0	-	-	-	-	-	-	23

[a] Reaction conditions: xylitol 10 wt.%, 135 mL solvent, 0,5 g 3.1%Ru/MnO(4.5%)/C, 60 bar H_2, 200°C; [b] at 60% conversion; [c] threitol, erythritol, BDO; [d] R_i: ratio of recovered MeOH, acetaldehyde, or methyl xyloside concentration to the initial concentration; [e] CH_3-Xylo.: methyl xyloside (1 g) in H_2O.

The influence of the primary or secondary nature of the alcohol was also investigated by comparison of the reaction in 90:10 vol.% H_2O:1-PrOH and in 90:10 vol.% H_2O:2-PrOH (**Figure 3.d,f**). The catalytic activity increased from 58 h^{-1} in H_2O:1-PrOH to 148 h^{-1} in H_2O:2-PrOH, which was close to the activity in pure water (220 h^{-1}). The distribution of products was different, depending on the alcohol. Best results were achieved in H_2O:1-PrOH, wherein the overall selectivity to glycols and glycerol was as high as 70%, while the selectivity to C4 and C5 alditols was of 8%. As outlined above, in that case the retro-aldol reaction was favored vs. decarbonylation and epimerization reactions. Surprisingly, in H_2O:2-PrOH solvent, the product distribution was the same as in pure water. The selectivity to glycols was of 45% and the one to C4 and C5 alditols of 20%. Thus, competitive decarbonylation, epimerization and retro-aldol reactions took place in H_2O:2-Pr-OH. Moreover, no deactivation of the Ru/MnO/C catalyst was observed in H_2O:2-PrOH. Xylitol conversion was complete after 30 h (**Figure 3.f**) and no coke was detected on the used catalyst by TGA analysis unlike for the one after hydrogenolysis in H_2O:1-PrOH (**Figure S4**). Only a small amount of 2-PrOH was consumed during the reaction and traces of acetone were temporarily analyzed in the liquid phase, which confirmed that (de)hydrogenation reactions may occur on metallic sites of Ru/MnO/C catalyst. According to the literature, acetone is more rapidly hydrogenated to 2-PrOH than aldehydes to primary alcohols over noble metal catalysts.[40] Furthermore, we investigated the influence of the addition of 10 vol.% acetone in water for xylitol hydrogenolysis. Acetone was rapidly and totally hydrogenated to 2-PrOH after 5 h, while xylitol was completely converted after 9 h (**Figure S5**).

Based on these results, acetone was hydrogenated to 2-PrOH and did not form coke on the catalyst surface, contrary to aldehydes. As proposed by Alcalá et al.[41], dehydrogenation of the α-H next to the carbonyl group of adsorbed aldehydes leads to the formation of an oxametallacycle with metallic sites, which could be the precursor to the oligomer and to the coke formation. The α-H atom is not present for ketones and the cleavage of a C-C bond is much more difficult. A mechanistic pathway was proposed for the degradation of primary and secondary alcohols and aldehydic compounds, which explains that Ru sites are poisoned in primary alcohols (**Scheme 2**). We assumed that the adsorption mode of the alcohol was independent of the nature (primary or secondary) of the alcohol; the O-H bond cleavage yields an adsorbed alkoxy intermediate (step 1), which is stabilized in the presence of chemisorbed water.[36,42] Then, the alkoxy moves to adopt a parallel mode of adsorption on Ru surface (step 2), to form an oxametallacycle $\eta^1\eta^2$ (C,O) by releasing α-H atoms (step 3). The energy for adsorption of this compound is the same from primary or secondary alcohols. Then, the reaction pathway is different depending on the nature of the alcohol. Indeed, for secondary alcohols, desorption of the oxametallacycle intermediate (step 4') forms a ketone as observed in our results. Conversely, the intermediate from primary alcohols may release the second α-H to form a less labile complex than ketones (step 4). The latter could then be polymerized to oligomers and lead to the poisoning of active sites. Moreover, we observed a faster deactivation in the presence of acetaldehyde than in the presence of EtOH, suggesting that fewer steps were necessary between the adsorption and the coke formation (step 1'') (**Scheme 2**).

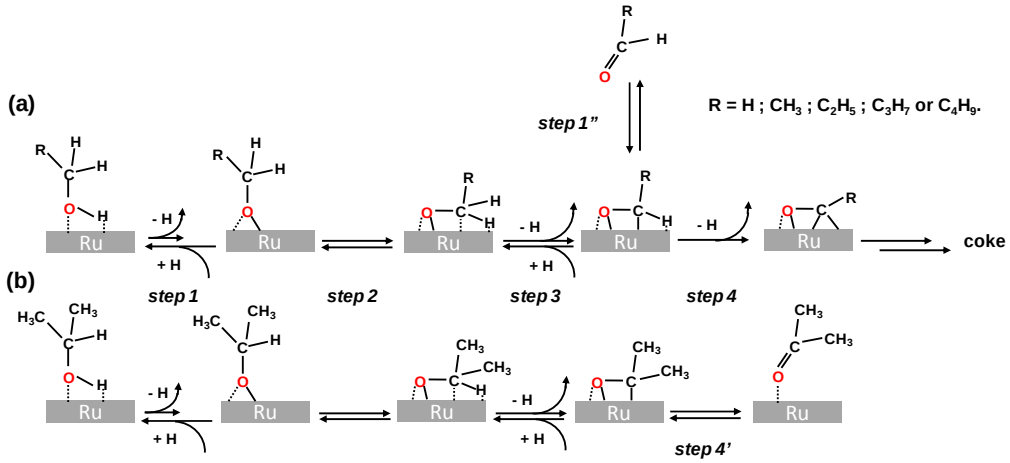

Scheme 2. Proposed mechanism pathways for (de)hydrogenation and coke formation on Ru sites of (a) primary alcohols and (b) secondary alcohols leading to selective poisoning of the catalyst. H_2O and H_2 not shown for clarity.

The clear differences in the results obtained in the different solvents confirm the presence of two types of active sites on the catalyst yielding different products. The metallic Ru sites are responsible for (de)hydrogenation and epimerization of xylitol (mostly to arabitol), as well as decarbonylation and dehydroxylation reactions producing C4 products and light alkanes by excessive C-C bond cleavage. The presence of MnO next to Ru particles generates less active bifunctional Ru-MnO active sites, on which successive (de)hydrogenation and retro-aldol reactions take place to produce glycols and glycerol. Therefore, the high selectivity to glycols and glycerol in 90:10 vol.% H_2O:ROH solvents can be explained by the selective poisoning of Ru sites, while the Ru-MnO sites are not affected. Afterwards, during the reaction the latter sites are also finally poisoned, and total catalyst deactivation is observed.

CONCLUSION

The solvent used for hydrogenolysis of xylitol over a bifunctional Ru/MnO/C catalyst at 200°C under 60 bar of H_2 has a significant influence on the product distribution. In 1,4-dioxane or 2-

PrOH aqueous solutions (90:10 vol.%) the catalyst behaved similarly as in pure water, namely it exhibited a high activity. Moreover, several reactions occurred competitively and yield light alkanes, BDO, C4 and C5 alditols on one hand, and EG, PG, and glycerol on the other hand. Conversely, in primary alcohol (MeOH, EtOH, 1-PrOH, 1-BuOH) aqueous solutions, a higher overall selectivity to glycols and glycerol (70%) was obtained at the expense of decarbonylation, dehydroxylation and epimerization reactions. Increasing the fraction of MeOH improved the selectivity to glycols, however, it accelerated the catalyst deactivation and the primary alcohol degradation. The deactivation was caused by dehydrogenation of the primary alcohol, which formed light alkanes (i.e. CH_4 from MeOH) and coke on the Ru surface. These results highlight the role of the primary alcohol in selective poisoning of Ru sites that are responsible for the side-reactions. In the meantime, the retro-aldol reaction takes place on the Ru-MnO sites, before being also deactivated.

AUTHOR INFORMATION

Corresponding Author

*to whom correspondence should be addressed. Email: michele.besson@ircelyon.univ-lyon1.fr Tel: +33 472 445 358.

ACKNOWLEDGMENT

The authors gratefully acknowledge financial support from Ecole Doctorale de Chimie Lyon (PhD grant M.R.) and IFP Energies nouvelles. The authors acknowledge the Service Scientifiques of IRCELYON for their help in the characterization of the catalyst.

REFERENCES

(1) Besson, M.; Gallezot, P.; Pinel, C. Conversion of biomass into chemicals over metal catalysts. *Chem. Rev.* **2014**, *114* (3), 1827–1870.

(2) Climent, M. J.; Corma, A.; Iborra, S. Converting carbohydrates to bulk chemicals and fine chemicals over heterogeneous catalysts. *Green Chem.* **2011**, *13* (3), 520–540.

(3) Petersen, G.; Werpy, T. *Top Value Added Chemicals from Biomass: Results of Screening for Potential Candidates from Sugars and Synthesis Gas, Vol I*; Springfield, 2004.

(4) Yue, H.; Zhao, Y.; Ma, X.; Gong, J. Ethylene glycol: properties, synthesis, and applications. *Chem. Soc. Rev.* **2012**, *41* (11), 4218–4244.

(5) Marinas, A.; Bruijnincx, P.; Ftouni, J.; Urbano, F. J.; Pinel, C. Sustainability metrics for a fossil- and renewable-based route for 1,2-propanediol production: A comparison. *Catal. Today* **2015**, *239*, 31–37.

(6) Zheng, M.; Pang, J.; Sun, R.; Wang, A.; Zhang, T. Selectivity control for cellulose to diols: Dancing on the eggs. *ACS Catal.* **2017**, *7* (3), 1939–1954.

(7) Jin, X.; Thapa, P. S.; Subramaniam, B.; Chaudhari, R. V. Kinetic Modeling of Sorbitol Hydrogenolysis over Bimetallic RuRe/C Catalyst. *ACS Sustain. Chem. Eng.* **2016**, *4* (11), 6037–6047.

(8) Hausoul, P. J. C.; Beine, A. K.; Neghadar, L.; Palkovits, R. Kinetics study of the Ru/C-catalysed hydrogenolysis of polyols – insight into the interactions with the metal surface. *Catal. Sci. Technol.* **2017**, *7* (1), 56–63.

(9) Jia, Y.; Liu, H. Mechanistic insight into the selective hydrogenolysis of sorbitol to propylene glycol and ethylene glycol on supported Ru catalysts. *Catal. Sci. Technol.* **2016**, *6*, 7042–7052.

(10) Montassier, C.; Ménézo, J. C.; Hoang, L. C.; Renaud, C.; Barbier, J. Aqueous polyol conversions on ruthenium and on sulfur-modified ruthenium. *J. Mol. Catal.* **1991**, *70* (1), 99–110.

(11) Sun, J.; Liu, H. Selective hydrogenolysis of biomass-derived xylitol to ethylene glycol and propylene glycol on supported Ru catalysts. *Green Chem.* **2011**, *13* (1), 135–142.

(12) Tajvidi, K.; Hausoul, P. J. C.; Palkovits, R. Hydrogenolysis of cellulose over Cu-based catalysts-analysis of the reaction network. *ChemSusChem* **2014**, *7* (5), 1311–1317.

(13) Deutsch, K. L.; Lahr, D. G.; Shanks, B. H. Probing the ruthenium-catalyzed higher polyol hydrogenolysis reaction through the use of stereoisomers. *Green Chem.* **2012**, *14* (6), 1635–1642.

(14) Liu, H.; Huang, Z.; Xia, C.; Jia, Y.; Chen, J.; Liu, H. Selective Hydrogenolysis of Xylitol to Ethylene Glycol and Propylene Glycol over Silica Dispersed Copper Catalysts Prepared by a Precipitation-Gel Method. *ChemCatChem* **2014**, *6*, 2918–2928.

(15) Huang, Z.; Chen, J.; Jia, Y.; Liu, H.; Xia, C.; Liu, H. Selective hydrogenolysis of xylitol to ethylene glycol and propylene glycol over copper catalysts. *Appl. Catal. B Environ.* **2014**, *147*, 377–386.

(16) Banu, M.; Sivasanker, S.; Sankaranarayanan, T. M.; Venuvanalingam, P. Hydrogenolysis of sorbitol over Ni and Pt loaded on NaY. *Catal. Commun.* **2011**, *12* (7), 673–677.

(17) Liu, H.; Huang, Z.; Kang, H.; Li, X.; Xia, C.; Chen, J.; Liu, H. Efficient bimetallic NiCu-SiO2 catalysts for selective hydrogenolysis of xylitol to ethylene glycol and propylene glycol. *Appl. Catal. B Environ.* **2018**, *220*, 251–263.

(18) Zhao, L.; Zhou, J. H.; Sui, Z. J.; Zhou, X. G. Hydrogenolysis of sorbitol to glycols over carbon nanofiber supported ruthenium catalyst. *Chem. Eng. Sci.* **2010**, *65* (1), 30–35.

(19) Rivière, M.; Perret, N.; Cabiac, A.; Delcroix, D.; Pinel, C.; Besson, M. Xylitol Hydrogenolysis over Ruthenium-Based Catalysts: Effect of Alkaline Promoters and Basic Oxide-Modified Catalysts. *ChemCatChem* **2017**, *9* (12), 2145–2159.

(20) Sun, J.; Liu, H. Selective hydrogenolysis of biomass-derived xylitol to ethylene glycol and propylene glycol on Ni/C and basic oxide-promoted Ni/C catalysts. *Catal. Today* **2014**, *234*, 75–82.

(21) Wang, X.; Liu, X.; Xu, Y.; Peng, G.; Cao, Q.; Mu, X. Sorbitol hydrogenolysis to glycerol and glycols over M-MgO (M = Ni, Co, Cu) nanocomposite: A comparative study of active metals. *Chinese J. Catal.* **2015**, *36* (9), 1614–1622.

(22) Murillo Leo, I.; López Granados, M.; Fierro, J. L. G.; Mariscal, R. Selective conversion of sorbitol to glycols and stability of nickel–ruthenium supported on calcium hydroxide catalysts. *Appl. Catal. B Environ.* **2016**, *185*, 141–149.

(23) Du, W. C.; Zheng, L. P.; Shi, J. J.; Xia, S. X.; Hou, Z. Y. Production of C2 and C3 polyols from D-sorbitol over hydrotalcite-like compounds mediated bi-functional Ni-Mg-Al-Ox catalysts. *Fuel Process. Technol.* **2015**, *139*, 86–90.

(24) Jin, X.; Shen, J.; Yan, W.; Zhao, M.; Thapa, P. S.; Subramaniam, B.; Chaudhari, R. V. Sorbitol Hydrogenolysis over Hybrid Cu/CaO-Al2O3 Catalysts: Tunable Activity and Selectivity with Solid Base Incorporation. *ACS Catal.* **2015**, *5* (11), 6545–6558.

(25) Mikkola, J.-P.; Salmi, T.; Sjöholm, R. Effects of solvent polarity on the hydrogenation of xylose. *J. Chem. Technol. Biotechnol.* **2001**, *76* (1), 90–100.

(26) Wang, C.; Jiang, H.; Chen, C.; Chen, R.; Xing, W. Solvent effect on hydrogenolysis of glycerol to 1,2-propanediol over Cu–ZnO catalyst. *Chem. Eng. J.* **2015**, *264*, 344–350.

(27) Capello, C.; Fischer, U.; Hungerbühler, K. What is a green solvent? A comprehensive framework for the environmental assessment of solvents. *Green Chem.* **2007**, *9* (9), 927–934.

(28) Ishikawa, M.; Tamura, M.; Nakagawa, Y.; Tomishige, K. Demethoxylation of guaiacol and methoxybenzenes over carbon-supported Ru–Mn catalyst. *Appl. Catal. B Environ.* **2016**, *182*, 193–203.

(29) Chen, X.; Wang, X.; Yao, S.; Mu, X. Hydrogenolysis of biomass-derived sorbitol to glycols and glycerol over Ni-MgO catalysts. *Catal. Commun.* **2013**, *39*, 86–89.

(30) Hausoul, P. J. C.; Negahdar, L.; Schute, K.; Palkovits, R. Unravelling the Ru□Catalyzed Hydrogenolysis of Biomass□Based Polyols under Neutral and Acidic Conditions.

ChemSusChem **2015**, *8*, 3323–3330.

(31) Al-Shaal, M. G.; Wright, W. R. H.; Palkovits, R. Exploring the ruthenium catalysed synthesis of γ-valerolactone in alcohols and utilisation of mild solvent-free reaction conditions. *Green Chem.* **2012**, *14* (5), 1260–1263.

(32) Hong, U. G.; Kim, J. K.; Lee, J.; Lee, J. K.; Song, J. H.; Yi, J.; Song, I. K. Hydrogenation of succinic acid to tetrahydrofuran (THF) over ruthenium–carbon composite (Ru–C) catalyst. *Appl. Catal. A Gen.* **2014**, *469*, 466–471.

(33) Hammond, C. Intensification studies of heterogeneous catalysts: probing and overcoming catalyst deactivation during liquid phase operation. *Green Chem.* **2017**, *19*, 2711–2728.

(34) Garcia-Muelas, R.; Li, Q.; López, N. Density Functional Theory Comparison of Methanol Decomposition and Reverse Reactions on Metal Surfaces. *ACS Catal.* **2015**, *5* (2), 1027–1036.

(35) Loffreda, D.; Michel, C.; Delbecq, F.; Sautet, P. Tuning catalytic reactivity on metal surfaces: Insights from DFT. *J. Catal.* **2013**, *308*, 374–385.

(36) Sinha, N. K.; Neurock, M. A first principles analysis of the hydrogenation of C1C4 aldehydes and ketones over Ru(0001). *J. Catal.* **2012**, *295*, 31–44.

(37) Iglesias, J.; Melero, J. A.; Morales, G.; Paniagua, M.; Hernandez, B. Dehydration of Xylose to Furfural in Alcohol Media in the Presence of Solid Acid Catalysts. *ChemCatChem* **2016**, *8* (12), 2089–2099.

(38) Perret, N.; Grigoropoulos, A.; Zanella, M.; Manning, T. D.; Claridge, J. B.; Rosseinsky, M. J. Catalytic Response and Stability of Nickel/Alumina for the Hydrogenation of 5-Hydroxymethylfurfural in Water. *ChemSusChem* **2016**, 1–12.

(39) Ibáñez, M.; Artetxe, M.; Lopez, G.; Elordi, G.; Bilbao, J.; Olazar, M.; Castaño, P. Identification of the coke deposited on an HZSM-5 zeolite catalyst during the sequenced pyrolysis–cracking of HDPE. *Appl. Catal. B Environ.* **2014**, *148–149*, 436–445.

(40) van Druten, G. M. ; Ponec, V. Hydrogenation of carbonylic compounds. *Appl. Catal. A Gen.* **2000**, *191* (1–2), 163–176.

(41) Alcalá, R.; Greeley, J.; Mavrikakis, M.; Dumesic, J. A. Density-functional theory studies of acetone and propanal hydrogenation on Pt(111). *J. Chem. Phys.* **2002**, *116* (20), 8973–8980.

(42) Michel, C.; Zaffran, J.; Ruppert, A. M.; Matras-Michalska, J.; Jedrzejczyk, M.; Grams, J.; Sautet, P. Role of water in metal catalyst performance for ketone hydrogenation: a joint experimental and theoretical study on levulinic acid conversion into gamma-valerolactone. *Chem. Commun.* **2014**, *50* (83), 12450–12453.

SUPPORTING INFORMATION. Characterization of the catalysts with the XRD patterns of fresh and used catalysts. Physicochemical properties of pure solvents and H_2 solubilization. TGA analysis and catalytic test of xylitol in 90:10 vol.% H_2O:2-PrOH solvent

SYNOPSIS A new catalytic system (Ru/MnO/C catalyst, H_2O:alcohol solvent) was studied which provides high selectivity to glycols in hydrogenolysis of sugar polyol xylitol.